Composites Science and Technology 128 (2016) 116–122

Contents lists available at ScienceDirect

Composites Science and Technology

journal homepage: http://www.elsevier.com/locate/compscitech

Reinforcement of lignin-based carbon fibers with functionalized carbon nanotubes

Shichao Wang, Zhe Zhou**, Hengxue Xiang, Wei Chen, Erqiang Yin, Tienkiang Chang, Meifang Zhu*

State Key Laboratory for Modification of Chemical Fibers and Polymer Materials, College of Materials Science and Engineering, Donghua University, Shanghai 201620, China

ARTICLE INFO

Article history:
Received 19 January 2016
Received in revised form
13 March 2016
Accepted 16 March 2016
Available online 19 March 2016

Keywords:
Carbon fibers
Recycling
Mechanical properties
Melt-spinning

ABSTRACT

In an effort to increase the mechanical properties of lignin-based carbon fibers, carbon nanotubes grafted with lignin (CNTs-g-L) were synthesized by grafting lignin molecular chains onto the surface of CNTs to improve the interfacial adhesion between CNTs and lignin chains. The addition of CNTs-g-L improved the melt spinnability of lignin, and continuously spooled Lignin/CNTs-g-L melt spun fibers and their carbonized fibers were obtained. The interaction between CNTs-g-L and lignin phases improved the thermal stability of lignin but disordered the graphitic structure of lignin-based carbon fibers. The well-orientated CNTs-g-L increased the tensile strength of lignin-based carbon fibers from 171.2 MPa to 289.3 MPa when 0.5% CNTs-g-L was incorporated. However, due to voids generated by the breakage of chemical links in the functionalized CNTs, the tensile strength of carbon fibers obtained thus decreased with further increases in the CNTs-g-L content.

1. Introduction

Lignin is an amorphous complex biopolymer with a heterogeneous structure derived mainly from *p*-coumaryl, coniferyl, and sinapyl alcohols [1]. As the only large-volume renewable feedstock composed of aromatics, lignin is considered the most attractive sustainable precursor for carbonaceous materials [2]. Among all carbonaceous materials, carbon fibers draw the most attention due to their high tensile strength and modulus. Currently, carbon fibers are mainly obtained from petroleum-based poly(acrylonitrile) (PAN) feedstock by a solution spinning method. High costs and environmental concerns restrict their further application in many fields, especially in the automotive industry [3]. Compared with PAN-based carbon fibers, lignin-based carbon fibers prepared from melt spinning show an unparalleled advantage in production costs and environmental concerns. However, poor melt spinnability and low mechanical properties hinder the development and application of lignin-based carbon fibers.

To solve the aforementioned bottlenecks, huge efforts have been focused on the improvement of the melt spinnability of lignin because fine precursors are necessary for the manufacture of carbon fibers. A conventional method of improving the spinnability of lignin is chemical modification, including acetylation [4], esterification [5], etherification [6] and graft polymerization [7]. Although the meltability can be improved to a certain extent, the spinnability is still far from satisfactory. Moreover, the cost of modification is relatively high, which is not suitable for the large-scale production of carbon fibers. Another inexpensive method that can be applicable for industrial production is the blending of lignin with other melt spinnable synthetic polymers. Poly(ethylene terephthalate) (PET), polypropylene (PP), poly(ethylene oxide) (PEO), and poly(-lactic acid) (PLA) are used to facilitate the melt spinning process of lignin [3,8–10]. Continuously spooled lignin/polymer fibers are obtained by melt spinning. However, synthetic polymers will degrade and generate voids in the fibers during the stabilization and carbonization processes, leading to poor mechanical properties of the carbon fibers.

By contrast, very few studies have focused on increasing the mechanical properties of lignin-based carbon fibers directly. In recent years, carbon nanotubes (CNTs) with high tensile strength and tensile modulus have been successfully applied to improve the mechanical properties of precursors and carbon fibers. Chae et al. [11] studied the stabilization and carbonization of gel spun PAN/

* Corresponding author.
** Corresponding author.
E-mail addresses: zzhe@dhu.edu.cn (Z. Zhou), zhumf@dhu.edu.cn (M. Zhu).

http://dx.doi.org/10.1016/j.compscitech.2016.03.018
0266-3538/

CNTs fibers and reported that the addition of 1 wt% CNTs enhanced the carbon fiber modulus by 49% and the strength by 64%. More recently, CNTs have also been introduced into the lignin phase to prepare lignin/CNT-based carbon fibers. Teng et al. [12] prepared electrospun softwood kraft lignin/CNT fibers and their carbonized products, with results showing that the tensile strength and modulus of carbonized lignin/CNT/PEO were lower than those of lignin/PEO carbon fiber mats in all cases, which was attributed to the poor interfacial interaction between CNTs and the surrounding matrix. Liu et al. [13] in their recent work also demonstrated that the addition of CNTs to PAN/lignin composites decreased the tensile strength and modulus of PAN/lignin-based carbon fibers. As in the case of electrospinning and gel spinning, a poor increase in mechanical properties was also found in melt spun lignin/CNT fibers. Although no original data were provided, Baker et al. [14] reported that at an optimal level of CNTs, the lignin/CNT-based carbon fibers exhibited only a 20% increase in tensile strength compared to that of neat lignin-based carbon fibers. The reason for this poor increase was also attributed to the low interfacial adhesion between non-functionalized CNTs and lignin carbons.

To improve the interfacial adhesion, CNTs were modified by grafting, a simple and powerful way of forming a continuous interphase between CNTs and the matrix [15,16]. In the present work, we designed the compatibilizer by grafting lignin chains onto the surface of CNTs (abbreviated as CNTs-g-L). Continuously spooled lignin/CNTs-g-L fibers were prepared by melt spinning. The interaction between CNTs-g-L and lignin, the morphology, and the mechanical properties of the obtained carbon fibers were investigated to obtain comprehensive knowledge of the preparation of lignin-based carbon fibers enhanced by a carbon material.

2. Experimental section

2.1. Materials

Hardwood kraft lignin (M_w = 4610, M_n = 3320) was kindly provided by Suzano Papel e Celulose S.A. Corp., Brazil. Lignin was purified using a ceramic membrane with a cut-off value of 0.05 μm, as described in our former work [3]. Industrial grade carboxyl multi-wall carbon nanotubes (−COOH content: 1.55%) were supplied by Chengdu Organic Chemicals Co. Ltd. (Chengdu, China). Methylenediphenyl diisocyanate (MDI), chloroform ($CHCl_3$), and dibutyltin dilaurate were purchased from Sinopharm Chemical Reagent Co., Ltd. (Shanghai, China) and used without further purification.

2.2. Synthesis of CNTs-g-L

The synthesis scheme of CNTs-g-L is illustrated in Fig. S1. Five grams of CNTs was swelled in 500 mL $CHCl_3$ in a four-necked round-bottom flask and sonicated for 40 min in an oil bath (50 °C). Two milliliters of MDI was added to the flask with continuous mechanical stirring for 1 h under a nitrogen atmosphere. After that, 3 g of purified lignin and two drops of catalyst (dibutyltin dilaurate) were added to the solution and reacted for another 3.5 h. The resulting solution was filtered and washed five times with $CHCl_3$ to remove unreacted lignin and other reagents before being collected and dried at 80 °C under vacuum overnight. Then, the dry CNTs-g-L were Soxhlet extracted for 48 h using $CHCl_3$ to remove adsorbed lignin before testing.

2.3. Preparation of lignin/CNTs-g-L fibers and their carbonized fibers

Lignin and CNTs-g-L powders were mixed together in an internal mixer at 220 °C for 5 min at a roller speed of 50 rpm. The CNTs-g-L contents used were 0, 0.5, 1, 2 and 3 wt% of the total weight, and the corresponding composites were labeled as lignin, lignin/0.5%CNTs-g-L, lignin/1%CNTs-g-L, lignin/2%CNTs-g-L and lignin/3%CNTs-g-L, respectively. All of the lignin/CNTs-g-L composites were fed into a twin screw micro-compounder equipped with a take-up device and processed at 225 °C. The obtained fibers were adhered to a ceramic ark and carbonized according to our former work [3]. The characterization methods of Lignin/CNTs-g-L composites and their carbonized fibers were supplied in the supplementary information.

3. Results and discussion

3.1. Structural characterization of CNTs-g-L

A valuable tool for estimating the species and amounts of hydroxyl (OH) relies on ^{31}P NMR analysis of lignin derivatized in situ by 2-chloro-4,4,5,5-tetramethyl-1,3,2-dioxaphospholane (TMDP) [17,18]. As shown in Fig. S2, aliphatic OH, syringyl (S) phenolic OH, guaiacyl (G) phenolic OH and carboxylic acid OH were seen in the purified lignin. The specific contents were calculated and are supplied in Table S1. Aliphatic OH and carboxylic OH from lignin and CNTs provided opportunities to react with NCO groups from carbon content-enriched MDI. To confirm our hypothesis, FTIR was used to elucidate the structural differences between unmodified CNTs and modified CNTs (Fig. 1). From Fig. 1(a), we can see that O—H stretching, C—H stretching and C═O stretching appeared in all of the spectra, although there are differences in their relative intensities. In contrast to CNTs, CNTs-g-L showed two remarkable peaks that appeared at 1512 cm^{-1} and 1113 cm^{-1}, which corresponded to functional groups in lignin (Fig. 1(b)). The appearance of a band at 1512 cm^{-1} was assigned to the characteristic vibration of the aromatic skeleton, while the absorption at 1113 cm^{-1} represented C—H stretching of the S ring and G ring [19]. In addition, the C—N stretching absorption was also found at 1402 cm^{-1} in CNTs-g-L samples.

To further investigate the structure of CNTs-g-L, XPS was used to measure the near-surface composition and examine the valence states of the observed elements [20]. As shown in Fig. 2(a), the XPS spectrum of unmodified CNTs showed only the presence of carbon and oxygen atoms. However, nitrogen atoms were clearly found in the spectrum of CNTs-g-L (Fig. 2(c)), and the calculated N/C atomic ratio was 0.023. In addition, the O/C atomic ratio increased from 0.032 in CNTs to 0.129 in CNTs-g-L. Fig. 2(b) shows the high-resolution XPS spectra of C 1s of CNTs. The strong C 1s peak (284.7 eV) corresponded to graphitic carbon, while the weaker peaks were assigned to C—O (286.2 eV) and −C—C* (292.6 eV). After modification, the peak intensity of 286.2 eV increased significantly (Fig. 2(d)), which was caused by the formation of C—N bonds and the contribution from C—O bonds that are present in high quantities in lignin. The results of FTIR and XPS demonstrate that lignin was successfully grafted onto the surface of CNTs.

3.2. Interaction between CNTs-g-L and lignin

The TG curves of CNTs, CNTs-g-L and their composites with lignin are shown in Fig. 3. The degradation parameters are summarized in Table 1, including the temperature at 5% weight loss ($T_{5\%}$) and the residual weight at 1000 °C (W_f). The weight loss of CNTs is due mainly to amorphous carbon and other impurities in CNTs [21]. Compared with unmodified CNTs, large mass loss in CNTs-g-L occurred when the temperature was above 260 °C because of the degradation of the propanoid side chains of lignin [22]. As a result, the $Ts_{5\%}$ of lignin and CNTs-g-L occurred at 316.5 °C

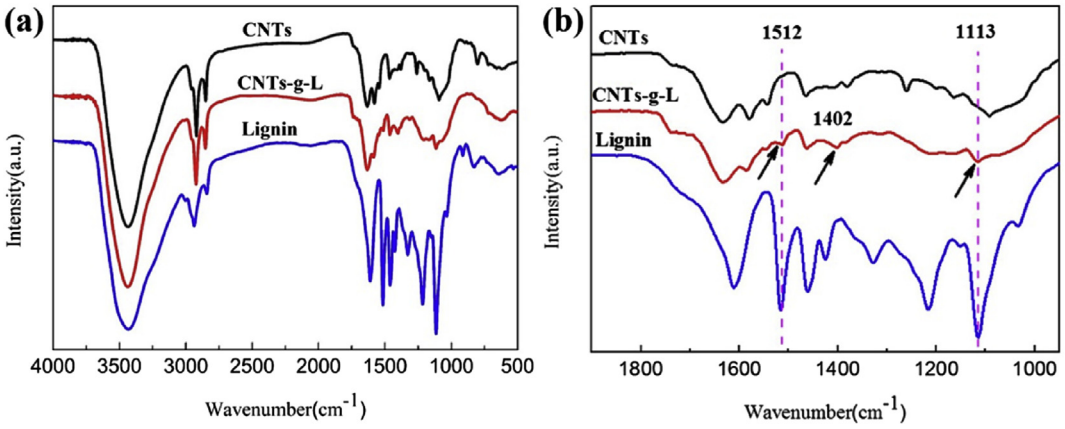

Fig. 1. FTIR spectra (a) and local amplification spectra (b) of CNTs, CNTs-g-L and lignin.

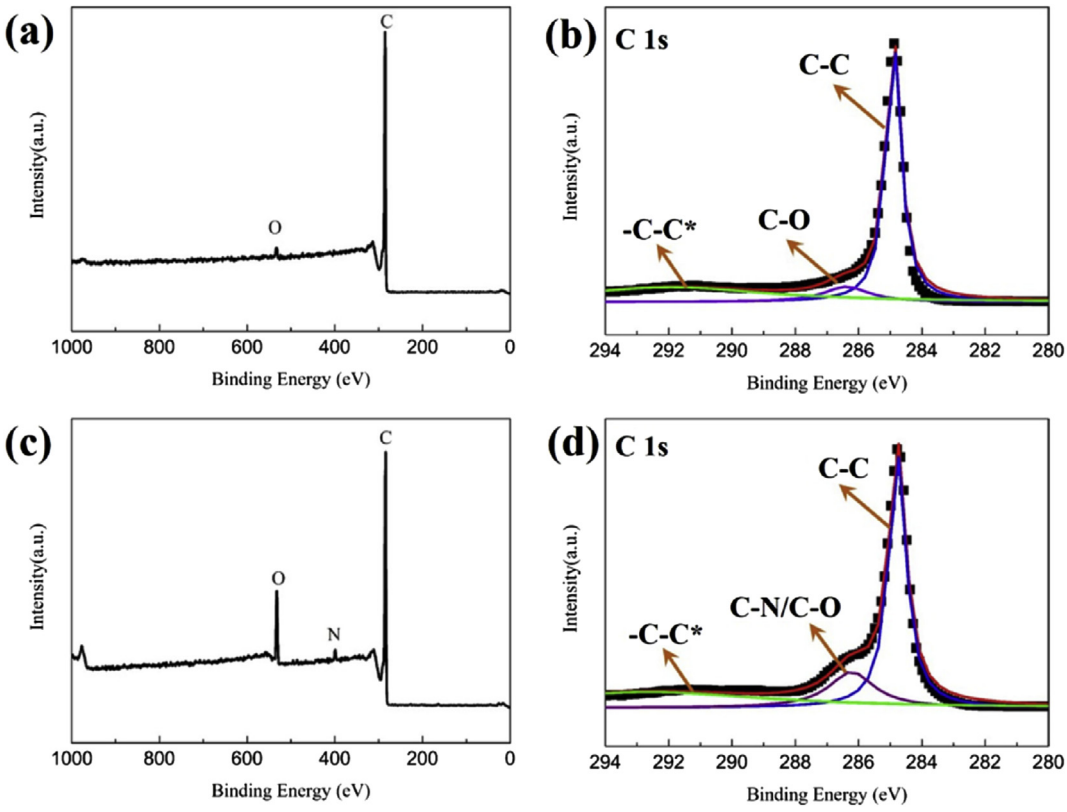

Fig. 2. XPS spectra of CNTs (a, b) and CNTs-g-L (c, d): (a, c) full survey spectrum, (b, d) high-resolution spectrum of C 1s.

and 304.7 °C, respectively (Table 1). In addition, the W_f also decreased from 75.7% for CNTs to 69.0% for CNTs-g-L. However, the $Ts_{5\%}$ increased to approximately 324 °C in the composites with CNTs-g-L, and the W_f also changed from 42.0% to 45.9% when 0.5% CNTs-g-L was incorporated into lignin. As a comparison, no significant changes in $T_{5\%}$ and W_f were observed in lignin/CNT composites when the CNT content was below 3%. This phenomenon implies that a strong interaction formed between lignin and CNTs-g-L, which also demonstrates that lignin was successfully grafted onto the surface of CNTs. After being grafted with lignin, the surface of CNTs was covered with lignin molecular chains, which improved the compatibility between CNTs and the lignin matrix. The close proximity between lignin and CNTs-g-L increased the π-π* interaction between the aromatic rings of lignin and CNTs [23]. As a result, the thermal stability and carbon residue rate of lignin/CNTs-g-L increased to a certain extent.

XRD patterns of lignin/CNTs-g-L-based carbon fibers are shown in Fig. 4(a). All of the samples exhibited two major diffraction peaks at 2θ~23° and 2θ~43°, corresponding to (002) and (100) planes of the graphitic crystalline structure, respectively [24]. The average interlayer spacing d_{002} and the crystallite dimensions L_{002} and L_{100} were calculated using the Bragg and Scherrer formulas and are listed in Table 2 [25]. d_{002} is an indication of the degree of alignment of the graphene planes within the graphitic structure, and the theoretical value of this interplanar spacing for an ideal graphite crystal is 0.335 nm [26]. The calculated d_{002} of lignin-based carbon

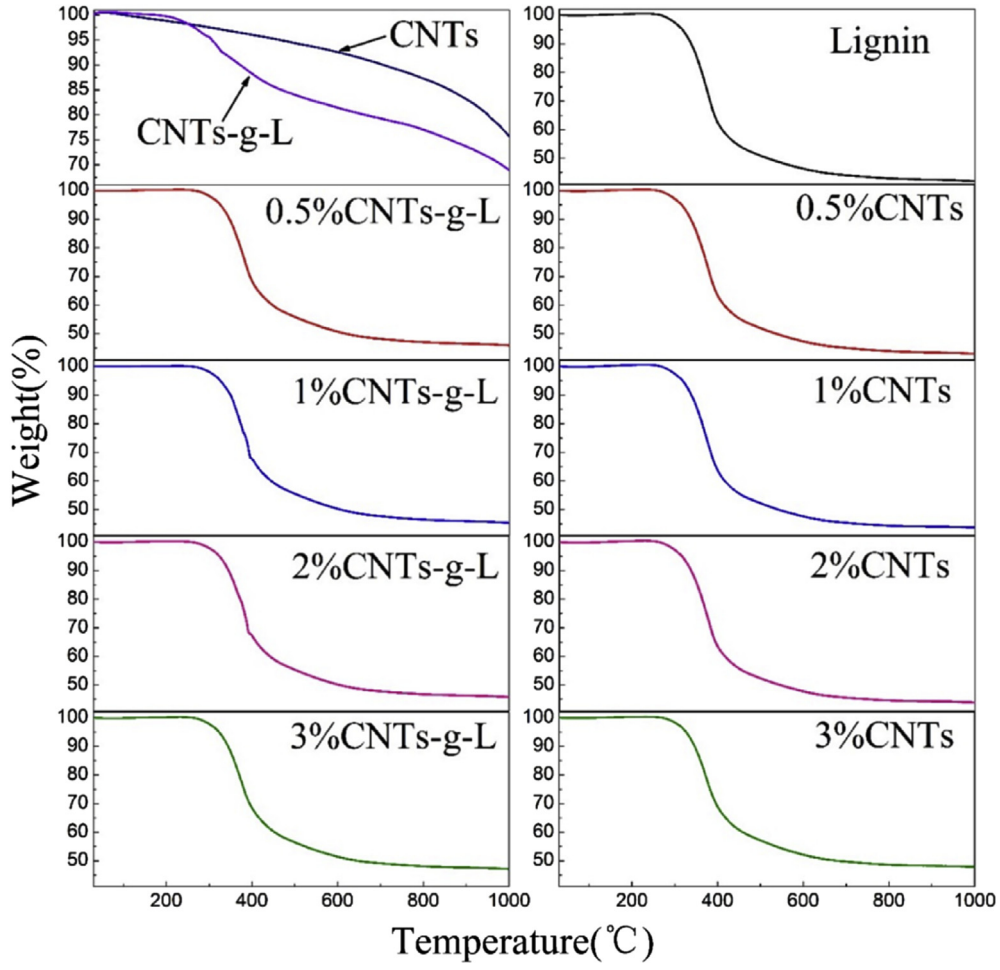

Fig. 3. TGA curves of CNTs, CNTs-g-L, lignin/CNTs-g-L (a) and lignin/CNTs composites (b).

Table 1
Degradation parameters obtained from TG curves.

Samples	$T_{5\%}$ (°C)	W_f (%)	Samples	$T_{5\%}$ (°C)	W_f (%)
Lignin	316.5	42.0			
0.5%CNTs-g-L	324.5	45.9	0.5%CNTs	316.4	43.0
1%CNTs-g-L	325.4	45.4	1%CNTs	317.6	43.7
2%CNTs-g-L	324.1	45.8	2%CNTs	316.0	43.9
3%CNTs-g-L	323.1	47.2	3%CNTs	326.1	47.9
CNTs-g-L	304.7	69.0	CNTs	462.9	75.7

Table 2
XRD and Raman data of lignin/CNTs-g-L-based carbon fibers.

Samples	d_{002} (nm)	L_{002} (nm)	L_{100} (nm)	I_D/I_G
Lignin	0.380	0.951	3.399	2.20
0.5%CNTs-g-L	0.402	1.093	3.457	2.40
1%CNTs-g-L	0.394	0.976	3.688	2.51
2%CNTs-g-L	0.398	1.059	3.518	2.44
3%CNTs-g-L	0.381	0.984	3.642	2.37

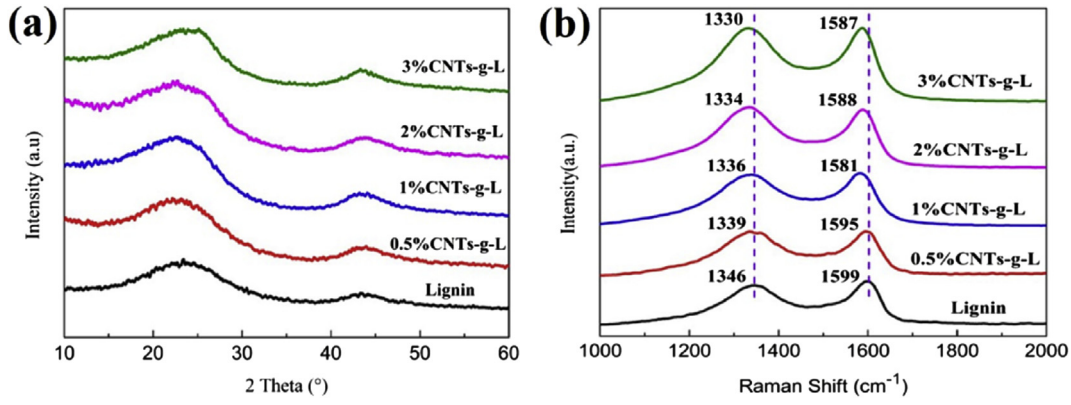

Fig. 4. XRD patterns and Raman spectra of lignin/CNTs-g-L-based carbon fibers.

fibers was 0.380 nm, suggesting a turbostratic carbon structure. However, the value increased when CNTs-g-L was incorporated into lignin. The decrease in the degree of alignment was caused by the translation or rotation of graphene layers [24], which demonstrated that a strong interaction existed between CNTs-g-L and the lignin phase. Additionally, the crystallite size of lignin-based carbon fibers was also increased by the addition of CNTs-g-L, as demonstrated by the increase in L_{002} and L_{100} of lignin/CNTs-g-L-based carbon fibers.

Raman spectroscopy was used to characterize the structure and quality of the obtained carbon materials, particularly the defects and the ordered or disordered structures of lignin/CNTs-g-L-based carbon fibers. As shown in Fig. 4(b), two overlapping broad peaks with intensity maxima at ~1340 cm^{-1} (D band, in the hybridized sp^3 valence state) and ~1590 cm^{-1} (G band, in the hybridized sp^2 valence state) can be observed, indicating that highly disordered carbon structure existed mainly as a form of sp^3 hybridization in lignin/CNTs-g-L-based carbon fibers [27]. The ratio of I_D/I_G of lignin-based carbon fibers was 2.20, which was lower than those of lignin/CNTs-g-L-based carbon fibers (Table 2), suggesting that the incorporation of CNTs-g-L disordered the graphitic structure of lignin-based carbon fibers. This result was consistent with that obtained from XRD. In addition, peak shifts of both the D and G bands were observed for the carbon fibers containing CNTs-g-L. As an example, the D band and G band of lignin-based carbon fibers shifted from 1346 cm^{-1}–1339 cm^{-1} and from 1599 cm^{-1}–1595 cm^{-1}, respectively, when 0.5% CNTs-g-L was incorporated. The downshift of the D and G peaks was due to an increase in the fraction of sp^3 carbon and the π-π^* interaction between lignin and CNTs-g-L [28,29].

3.3. Morphology and mechanical properties of carbonized fibers

Continuously spooled lignin and lignin/CNTs-g-L fibers are shown in Fig. 5(a). At an optimal level of CNTs-g-L, the addition of CNTs-g-L increased the melt spinnability compared with lignin via the increased heat capacity of composites, which allowed the fibers to remain molten at a greater distance on the spin-line [14]. Fig. 5(b) shows the surface morphology of carbonized fibers. The surface of lignin-based carbon fibers was smooth, while that of lignin/CNTs-g-L based carbon fibers became rough and the roughness increased with increasing CNTs-g-L content. The cross-section morphology of obtained carbon fibers is shown in Fig. 5(c). Some voids appeared in the lignin-based carbon fibers, which was caused by the volatilization of carbohydrates during the stabilization and carbonization processes. When 0.5% CNTs-g-L was added to lignin, much more voids were generated in the internal carbonized fibers and the situation became worse as the CNTs-g-L content increased. As a comparison, the morphology of lignin/CNT-based carbon fibers is described in Fig. S3. In contrast to the modified CNTs, the void content was almost unchanged with increasing amounts of added CNTs. This comparison suggests that the voids in lignin/CNTs-g-L-based carbon fibers are mainly caused by the modification of CNTs. The chemical linkages between CNTs and lignin may break during the stabilization and carbonization processes due to the high temperature, which accelerates the formation of volatiles and the appearance of voids in the carbon fibers. Further work was carried out to study the formation stage and the controllability of voids that appeared in lignin/3%CNTs-g-L-based carbon fibers, as shown in Fig. S4. When the stabilization temperature reached 260 °C, a small number of voids appeared in the edge of the fibers (Fig. S4(a)). The number of voids remained almost the same until the temperature rose to 280 °C (Fig. S4(b)). However, many more voids were generated after 1 h of stabilization at 280 °C (Fig. S4(c)). The stabilized fibers were then heated to 1000 °C at a rate of 5 °C/min, and the number of voids further increased (Fig. S4(d)). However, the amount of void space was less than that obtained at a rate of 3 °C/min (Fig. 5(c)). Similar phenomena can also be found when the heating rate of stabilization changed to 0.1 °C/min (Fig. S4(e),(g),(h)). Surprisingly, most of the voids disappeared after carbonization under the heating rate of 1 °C/min (Fig. S4(f)). Based on these results, we believe that the voids are mainly formed during the last stage of the stabilization process and that the amount of void space can be controlled by optimizing the process conditions.

The tensile strength and tensile modulus of lignin/CNTs-g-L- and lignin/CNTs-based carbon fibers are shown in Fig. 6(a) and Fig. 6(b), respectively. Because no tension was applied to lignin fibers during the carbonization process, the mechanical properties of such obtained carbon fibers were lower than those reported by Kubo [8]. The tensile modulus of lignin/CNTs-g-L-based carbon fibers changed slightly, suggesting that the addition of CNTs-g-L had little effect on the orientation of graphite crystallite. However, the tensile strength increased significantly when incorporated with

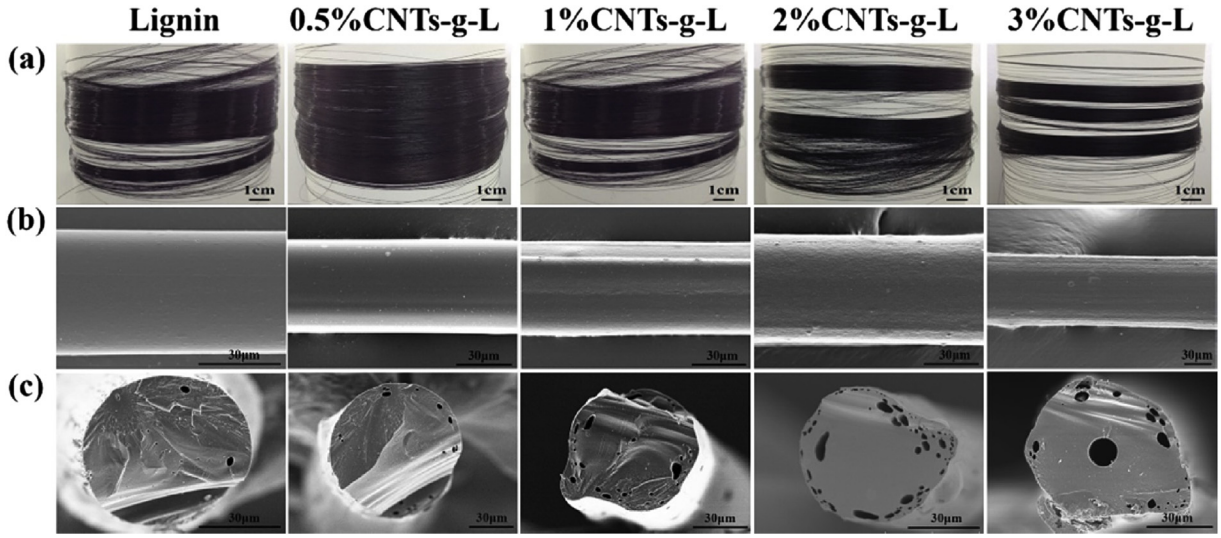

Fig. 5. Continuously spooled lignin/CNTs-g-L fibers and their carbonized fibers. Lignin/CNTs-g-L fibers spooled on cylinders (a); surface morphology (b) and cross-sectional morphology (c) of lignin/CNTs-g-L-based carbon fibers.

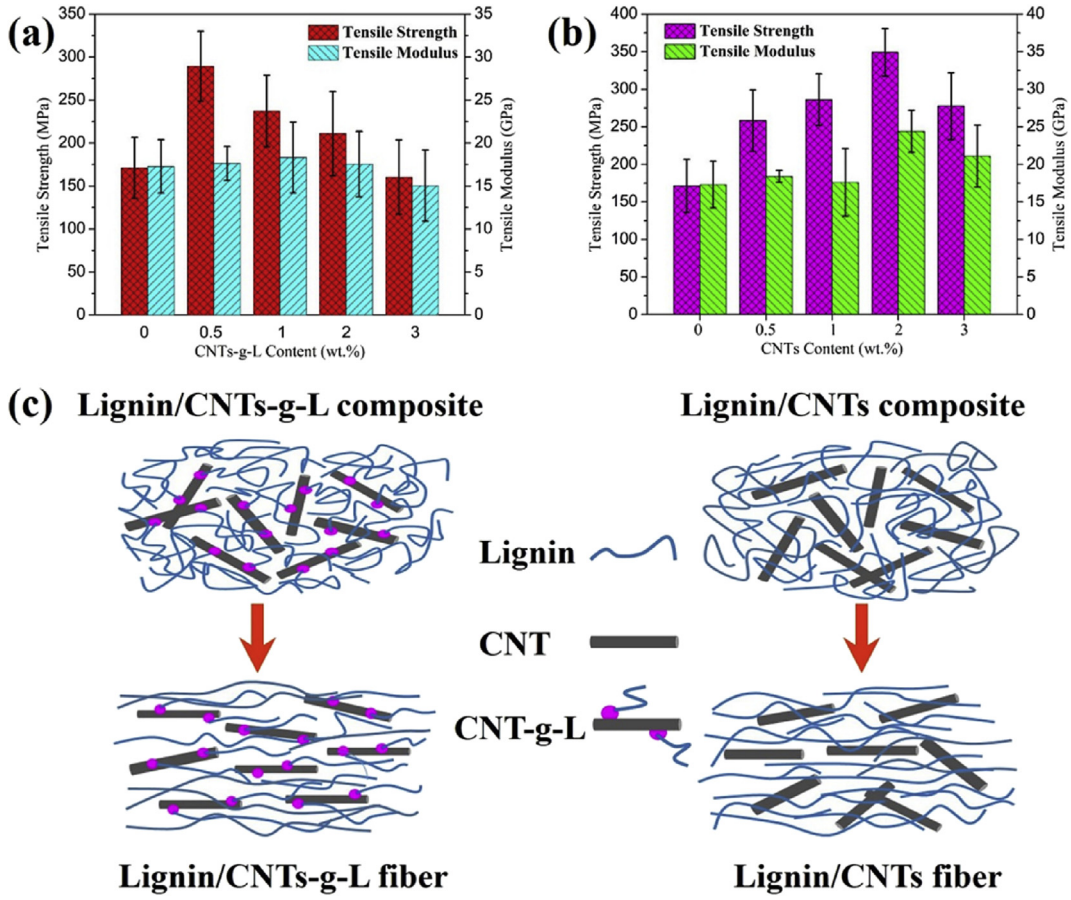

Fig. 6. Mechanical properties of lignin/CNTs-g-L- (a) and lignin/CNT-based carbon fibers (b) and a schematic diagram of the orientation of CNTs-g-L and CNTs (c).

CNTs-g-L. For example, the tensile strength increased from 171.2 MPa for lignin-based carbon fibers to 289.3 MPa for lignin/0.5%CNTs-g-L-based carbon fibers when only 0.5% CNTs-g-L was incorporated. However, the tensile strength showed a decreasing trend with increasing CNTs-g-L content due to the formation of voids in the carbon fibers. When comparing Fig. 6(a) and (b), it can be found that the filler content corresponding to the optimal properties was 0.5% for modified CNTs and 2% for unmodified CNTs. The increased compatibility between CNTs-g-L and the lignin phase and the strong π-π^* interaction afford CNTs-g-L alignment during the fiber formation process and, at the same time, pull lignin molecular chains in the matrix to orientate along the fiber axis. As shown in Fig. S5, all of the CNTs-g-L observed were perpendicular to the cross-section of lignin/CNTs-g-L-based carbon fibers. Thus, strong interfacial adhesion and well-orientated lignin/CNTs-g-L-based carbon fibers were obtained (Fig. S6(a)), which was effective in improving the tensile strength. On the other hand, the increase in CNTs-g-L generated more voids, and the tensile strength became more dependent on the weak-link effect. As a result, the optimal properties were obtained at a CNTs-g-L content of 0.5%. For unmodified CNTs, the weak interaction between CNTs and lignin resulted in low interfacial adhesion between CNTs and lignin carbons, as shown in Fig. S6(b). Due to decreased interaction between CNTs and lignin, the contribution of the CNTs in the orientation phenomenon was less effective than that of modified CNTs (as illustrated in Fig. 6(c)), leading to a lower tensile strength (258.2 MPa) than that of lignin/CNTs-g-L-based carbon fibers with 0.5% fillers. The maximum tensile strength was obtained at 2% CNTs when the fillers were interconnected, as verified by the results of electrical conductivity. As shown in Fig. S7, when the content of CNTs was less than 2%, the electrical conductivity of lignin/CNT-based carbon fibers increased due to the incorporation of CNTs with high electrical conductivity. After that, the CNT content was high enough to form a continuous pathway, and the electrical conductivity remained almost unchanged. However, increasing the amount of CNTs produces more defects on the surface of carbonized fibers. Therefore, optimal mechanical properties were observed in lignin/2%CNTs-based carbon fibers.

4. Conclusions

The compatibilizer CNTs-g-L was successfully synthesized by grafting lignin molecular chains onto the surface of CNTs. The structure of CNTs-g-L and the interaction between CNTs-g-L and the lignin phase were intensively characterized and analyzed. The results show that the strong interaction increased the thermal stability of lignin/CNTs-g-L composites but disordered the graphitic structure of lignin-based carbon fibers. The addition of CNTs-g-L improved the melt spinnability of lignin, and continuously spooled lignin/CNTs-g-L fibers were obtained. After the stabilization and carbonization processes, well-orientated CNTs-g-L increased the tensile strength of lignin-based carbon fibers from 171.2 MPa to 289.3 MPa when 0.5% CNTs-g-L was incorporated, which exceeded the tensile strength of lignin/CNT-based carbon fibers with 1% unmodified CNTs. However, many voids appeared in the carbonized lignin/CNTs-g-L fibers, which were generated by the breakage of chemical links between CNTs and lignin, decreasing the tensile strength of obtained carbon fibers. The generation of voids

can be controlled by optimizing the stabilization and carbonization processes, and further work is ongoing to synthesize an appropriate compatibilizer that will minimize void formation.

Acknowledgements

This research was financially supported by the Program for Changjiang Scholars and Innovative Research Team in University (T2011079, IRT1221), the Open Project of State Key Laboratory for Modification of Chemical Fibers and Polymer Materials, Donghua University (LK1407), and the China Postdoctoral Science Foundation (2015M581498).

Appendix A. Supplementary data

Supplementary data related to this article can be found at http://dx.doi.org/10.1016/j.compscitech.2016.03.018.

References

[1] J. Zakzeski, P.C.A. Bruijnincx, A.L. Jongerius, B.M. Weckhuysen, The catalytic valorization of lignin for the production of renewable chemicals, Chem. Rev. 110 (6) (2010) 3552–3599.
[2] S. Chatterjee, T. Saito, Lignin-derived advanced carbon materials, ChemSusChem. 8 (23) (2015) 3941–3958.
[3] S. Wang, Y. Li, H. Xiang, Z. Zhou, T. Chang, M. Zhu, Low cost carbon fibers from bio-renewable Lignin/Poly(lactic acid) (PLA) blends, Compos. Sci. Technol. 119 (2015) 20–25.
[4] M. Zhang, A.A. Ogale, Carbon fibers derived from acetylated softwood kraft lignin, in: A.K. Naskar, W.P. Hoffman (Eds.), Polymer Precursor-Derived Carbon, 1173, 2014, pp. 137–152.
[5] M. Thunga, K. Chen, D. Grewell, M.R. Kessler, Bio-renewable precursor fibers from lignin/polylactide blends for conversion to carbon fibers, Carbon 68 (2014) 159–166.
[6] J. Lin, K. Koda, S. Kubo, T. Yamada, M. Enoki, Y. Uraki, Improvement of mechanical properties of softwood lignin-based carbon fibers, J. Wood Chem. Technol. 34 (2) (2014) 111–121.
[7] S.L. Hilburg, A.N. Elder, H. Chung, R.L. Ferebee, M.R. Bockstaller, N.R. Washburn, A universal route towards thermoplastic lignin composites with improved mechanical properties, Polymer 55 (4) (2014) 995–1003.
[8] S. Kubo, J. Kadla, Lignin-based carbon fibers: effect of synthetic polymer blending on fiber properties, J. Polym. Environ. 13 (2) (2005) 97–105.
[9] S. Kubo, T. Yoshida, J.F. Kadla, Surface porosity of lignin/PP blend carbon fibers, J. wood Chem. Technol. 27 (3–4) (2007) 257–271.
[10] J.F. Kadla, S. Kubo, R.A. Venditti, R.D. Gilbert, A.L. Compere, W. Griffith, Lignin-based carbon fibers for composite fiber applications, Carbon 40 (15) (2002) 2913–2920.
[11] H.G. Chae, M.L. Minus, A. Rasheed, S. Kumar, Stabilization and carbonization of gel spun polyacrylonitrile/single wall carbon nanotube composite fibers, Polymer 48 (13) (2007) 3781–3789.
[12] N.-Y. Teng, I. Dallmeyer, J.F. Kadla, Incorporation of multiwalled carbon nanotubes into electrospun softwood kraft lignin-based fibers, J. Wood Chem. Technol. 33 (4) (2013) 299–316.
[13] H.C. Liu, A.T. Chien, B.A. Newcomb, Y.D. Liu, S. Kumar, Processing, structure, and properties of lignin- and CNT-incorporated polyacrylonitrile-based carbon fibers, Acs Sustain. Chem. Eng. 3 (9) (2015) 1943–1954.
[14] D.A. Baker, T.G. Rials, Recent advances in low-cost carbon fiber manufacture from lignin, J. Appl. Polym. Sci. 130 (2) (2013) 713–728.
[15] H.-Y. Yu, Z.-Y. Qin, B. Sun, X.-G. Yang, J.-M. Yao, Reinforcement of transparent poly(3-hydroxybutyrate-co-3-hydroxyvalerate) by incorporation of functionalized carbon nanotubes as a novel bionanocomposite for food packaging, Compos. Sci. Technol. 94 (2014) 96–104.
[16] H.-Y. Yu, Z.-Y. Qin, C.-F. Yan, J.-M. Yao, Green nanocomposites based on functionalized cellulose nanocrystals: A study on the relationship between interfacial interaction and property enhancement, Acs Sustain. Chem. Eng. 2 (4) (2014) 875–886.
[17] Y. Pu, S. Cao, A.J. Ragauskas, Application of quantitative P-31 NMR in biomass lignin and biofuel precursors characterization, Energy & Environ. Sci. 4 (9) (2011) 3154–3166.
[18] A. Granata, D.S. Argyropoulos, 2-Chloro-4,4,5,5-tetramethyl-1,3,2-dioxaphospholane, A reagent for the accurate determination of the uncondensed and condensed phenolic moieties in lignins, J. Agric. Food Chem. 43 (6) (1995) 1538–1544.
[19] K.K. Pandey, A study of chemical structure of soft and hardwood and wood polymers by FTIR spectroscopy, J. Appl. Polym. Sci. 71 (12) (1999) 1969–1975.
[20] Z. Geng, L. Wangting, C. Feifei, X. Zhidong, Z. Xinsheng, N-doped graphene coupled with Co nanoparticles as an efficient electrocatalyst for oxygen reduction in alkaline media, J. Power Sources 302 (2016) 114–125.
[21] L. Min, C. Meirong, W. Zhishen, L. Jianxun, Carbon nanotube grafted with polyalcohol and its influence on the thermal conductivity of phase change material, Energy Convers. Manag. 83 (2014) 325–329.
[22] M. Brebu, C. Vasile, Thermal degradation of lignin-A review, Cellul. Chem. Technol. 44 (9) (2010) 353–363.
[23] L. Wanshuang, Z. Rui, Z. Dan, D. Guoqiang, S. Jie Miin, Y. Chee Yoon, et al., Lignin-assisted direct exfoliation of graphite to graphene in aqueous media and its application in polymer composites, Carbon 83 (2015) 188–197.
[24] Z.Q. Li, C.J. Lu, Z.P. Xia, Y. Zhou, Z. Luo, X-ray diffraction patterns of graphite and turbostratic carbon, Carbon 45 (8) (2007) 1686–1695.
[25] M. Endo, C. Kim, T. Karaki, T. Kasai, M.J. Matthews, S.D.M. Brown, et al., Structural characterization of milled mesophase pitch-based carbon fibers, Carbon 36 (11) (1998) 1633–1641.
[26] W. Qin, J. Kadla, Effect of organoclay reinforcement on lignin-based carbon fibers, Ind. Eng. Chem. Res. 50 (22) (2011) 12548–12555.
[27] Y. Li, D. Cui, Y. Tong, L. Xu, Study on structure and thermal stability properties of lignin during thermostabilization and carbonization, Int. J. Biol. Macromol. 62 (2013) 663–669.
[28] J. Robertson, Diamond-like amorphous carbon, Mater. Sci. Eng. R Rep. R37 (2002) 4–6 cpp.1–281.
[29] M. Canetti, F. Bertini, Supermolecular structure and thermal properties of poly(ethylene terephthalate)/lignin composites, Compos. Sci. Technol. 67 (15–16) (2007) 3151–3157.